

## Influence of gas conditions on parameters of plasma jets generated in the PF-1000U plasma-focus facility

E. Skladnik-Sadowska, S. A. Dan'ko, A. M. Kharrasov, V. I. Krauz, R. Kwiatkowski, M. Paduch, M. J. Sadowski, D. R. Zaloga, and E. Zielinska

Citation: *Physics of Plasmas* **25**, 082715 (2018); doi: 10.1063/1.5045290

View online: <https://doi.org/10.1063/1.5045290>

View Table of Contents: <http://aip.scitation.org/toc/php/25/8>

Published by the [American Institute of Physics](#)

---

### Articles you may be interested in

[Observations of the magneto-Rayleigh-Taylor instability and shock dynamics in gas-puff Z-pinch experiments](#)  
*Physics of Plasmas* **25**, 072701 (2018); 10.1063/1.5032084

[Increasing stagnation pressure and thermonuclear performance of inertial confinement fusion capsules by the introduction of a high-Z dopant](#)

*Physics of Plasmas* **25**, 080706 (2018); 10.1063/1.5033459

[Magnetised thermal self-focusing and filamentation of long-pulse lasers in plasmas relevant to magnetised ICF experiments](#)

*Physics of Plasmas* **25**, 092701 (2018); 10.1063/1.5049229

[Axial compression of plasma structures in a plasma focus discharge](#)

*Physics of Plasmas* **25**, 062712 (2018); 10.1063/1.5033997

[Generation of keV hot near-solid density plasma states at high contrast laser-matter interaction](#)

*Physics of Plasmas* **25**, 083103 (2018); 10.1063/1.5027463

[Announcement: The 2017 Ronald C. Davidson Award for Plasma Physics](#)

*Physics of Plasmas* **25**, 083503 (2018); 10.1063/1.5049502

---

PHYSICS TODAY

WHITEPAPERS

MANAGER'S GUIDE

Accelerate R&D with  
Multiphysics Simulation

READ NOW

PRESENTED BY

 COMSOL

# Influence of gas conditions on parameters of plasma jets generated in the PF-1000U plasma-focus facility

E. Składnik-Sadowska,<sup>1</sup> S. A. Dan'ko,<sup>2</sup> A. M. Kharrasov,<sup>2,3</sup> V. I. Krauz,<sup>2,3</sup> R. Kwiatkowski,<sup>1</sup> M. Paduch,<sup>4</sup> M. J. Sadowski,<sup>1,4</sup> D. R. Zaloga,<sup>1</sup> and E. Zielinska<sup>4</sup>

<sup>1</sup>National Centre for Nuclear Research (NCBJ), A. Soltana 7, 05-400 Otwock-Świerk, Poland

<sup>2</sup>National Research Centre Kurchatov Institute, pl. Akademika Kurchatova 1, 123182 Moscow, Russia

<sup>3</sup>Moscow Institute of Physics and Technology, Institutsky per. 9, 141700 Dolgoprudny, Russia

<sup>4</sup>Institute of Plasma Physics and Laser Microfusion (IFPiLM), Hery 23, 01-497 Warsaw, Poland

(Received 19 June 2018; accepted 12 August 2018; published online 28 August 2018)

Several series of high-current discharges were carried out within the PF-1000U facility at various gas conditions. The initial filling pressures were  $p_0 = 1.2$  hPa  $D_2$ , 1.06 hPa  $D_2 + 10\%$  He, or 0.53 hPa  $D_2 + 25\%$  Ne. The discharges were performed with or without an additional gas puffing. In shots with the puffing,  $1\text{ cm}^3$  of gas (or mixture), compressed to the pressure of (0.13–0.20) MPa, was injected 1.5 ms before the discharge initiation. Pure  $D_2$ , He, Ne, or a mixture of 50% He + 50% Ne was used for puffing. The optical spectroscopic measurements were performed at a distance of 16 or 27 cm from the electrode outlets. Almost all discharges produced a dense plasma-focus (of about 10 cm in length) and a long plasma jet, which was observed for several  $\mu\text{s}$ . The ambient plasma density at the investigated gas-conditions was about  $10^{16}\text{ cm}^{-3}$ , but an admixture of 10% He or 25% Ne (added to the  $D_2$ -filling) induced an increase in this density by factor 1.8–2.5. In all the cases, the plasma jet density was above 10-times higher than that of ambient plasma. At the He- or Ne-puffing, this density reached  $(3.5\text{--}6) \times 10^{17}\text{ cm}^{-3}$ . Electron temperatures in the plasma jet changed from about 5.0 to about 3 eV in 5–7  $\mu\text{s}$ . *Published by AIP Publishing.*

<https://doi.org/10.1063/1.5045290>

## I. INTRODUCTION

Intense plasma jets of gigantic dimensions have been observed in cosmic space by many astrophysicists.<sup>1–7</sup> These astrophysical jets constitute astronomical phenomena in which large outflows of ionized matter are emitted as very extended beams. Such jets can extend from thousands up to millions of parsecs. Their generation is not well understood, but according to several physical models, they probably arise from interactions within accretion disks and from processes within compact central objects as black holes, neutron stars, or pulsars. When the accelerated matter approaches the speed of light, the astrophysical jets become relativistic ones and demonstrate some relativistic effects. Such jets cannot of course be produced on the Earth, but some researchers showed that the plasma phenomena observed in nonrelativistic jets can be simulated in a laboratory at an appropriate scaling.<sup>8–13</sup> For this purpose, the use was made of pulsed Z-pinch discharges<sup>12</sup> as well as powerful lasers<sup>13</sup> and other plasma facilities. In recent years, particular attention has been focused on the dense plasma jets produced by high-current discharges of the plasma-focus type.<sup>14–18</sup>

Experimental studies, as carried out with the PF-3 facility at the Kurchatov Institute,<sup>14,15,17,19,20</sup> showed that plasma-focus discharges produce plasma jets, which can propagate along the axis up to distances much greater than their transverse dimensions. Those plasma jets achieved velocity  $v > 10^7$  cm/s, the Mach number  $M > 1$ , the ratio the jet density to that of ambient plasma (a so-called contrast)  $K = 10$ , the Reynolds number  $Re = 10^4\text{--}10^5$ , and the

electron temperature  $T = 3\text{--}8$  eV, i.e., parameters which are of interest for the simulation of non-relativistic astrophysical jets emitted from young stellar objects (YSO).

Preliminary studies of dense plasma jets were also performed within a modernized PF-1000U facility at the IFPiLM in Poland.<sup>16,17</sup> On the basis of the recorded magnetic probes signals, it was deduced that the plasma stream achieved velocity  $v = 4 \times 10^6$  cm/s at a distance of 60 cm from the electrode outlets, and the Mach number was  $M > 2$ . Earlier measurements, which were performed with a laser interferometer,<sup>17</sup> showed that the dense pinch core (of about 2 cm in diameter, and about 10 cm in length) had an electron density ranging from  $5 \times 10^{18}$  to  $2 \times 10^{19}\text{ cm}^{-3}$ . Using the optical emission spectroscopy (OES) techniques,<sup>21,22</sup> from spectral measurements performed at a distance of about 60 cm from the electrodes outlets it was estimated that the plasma density in jets was equal to  $(0.3\text{--}3) \times 10^{17}\text{ cm}^{-3}$ , and densities of ambient plasma were one order of magnitude lower. Hence, the contrast was equal to  $K \approx 6$ , and the Reynolds number achieved the value of  $Re > 2 \times 10^4$ . For deuterium discharges with the additional helium puffing, on the basis of the measured ratio of *He II* 468.6 nm and *He I* 587.6 nm intensities, it was estimated that the electron temperature inside the plasma jet was about 5.3 eV. The determined parameters seemed also to be perspective for simulation of the non-relativistic astrophysical jets, but the data were obtained at one plane only (at a distance  $z = 57$  cm). Therefore, it appeared reasonable to perform more detailed spectroscopic measurements within the PF-1000U facility under different operational conditions.

The main aim of several series of new experiments within the PF-1000U device was to perform detailed OES measurements of electron densities and temperatures in plasma jets and ambient plasmas at other distances from the electrode outlets and at various gas conditions.

## II. EXPERIMENTAL SETUP

The reported experiments were performed in the large PF-1000U facility, which similarly to the previous studies<sup>16</sup> was equipped with coaxial electrodes of 46 cm in length. The outer electrode (cathode) was composed of 12 stainless-steel tubes (each of 8 cm in diameter) distributed symmetrically around a cylindrical surface of 40 cm in diameter. The inner electrode (anode) was a thick-wall 23-cm-diam. copper-tube ended by a thick copper-plate with an axial 5-cm-diam. hole, which was used for the axial gas-puffing by means of a fast electro-dynamic valve. Those electrodes were connected with the main current-collector fixed to one end of a large vacuum chamber of 1.4 m in diameter and 2.5 m in length. The experimental arrangement and a general view of the PF-1000U facility are shown in Fig. 1.

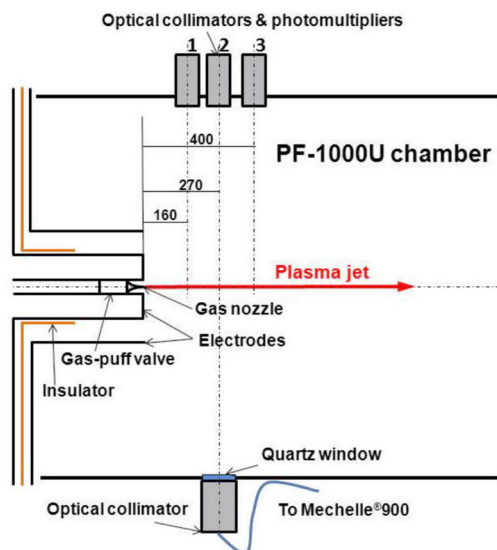


FIG. 1. Scheme of the experimental setup, which was used for studies of plasma jets and a general view of the PF-1000U facility.

During the described experiments, the PF-1000U chamber was filled up with a pure deuterium ( $D_2$ ) up to the initial pressure  $p_0 = 1.2$  hPa, or with a mixture of  $D_2$  and helium (He) or neon (Ne). Many discharges were performed with the additional puffing of a chosen gas ( $D_2$ , He, Ne, or their mixture). In such a case,  $1 \text{ cm}^3$  of the chosen gas (or mixture), compressed to the pressure of (0.13–0.20) MPa, was injected by the fast valve along the  $z$ -axis, about 1.5 ms before triggering of the main discharge. All the discharges, as carried out during the reported experimental series, were powered from a condenser bank of the total capacity  $C_0 = 1.33$  mF, which was charged to the initial voltage  $U_0 = 16$  kV and stored energy  $E_0 = 170$  kJ. The peak current reached 1.2–1.5 MA, and the current during the pinch phase was about 1 MA.

To perform OES measurements, a quartz window and an optical collimator were located on the side-wall of the vacuum chamber, at the plane  $z = 16$  cm or 27 cm from the end plane of the electrodes outlets. That collimator was coupled (through an optical cable) with the input of the Mechelle<sup>®</sup>900 spectrometer, which could record spectra in the wavelength range from 300 nm to about 1100 nm, with an exposition time adjustable from 100 ns to 50 ms. The spectrometer gate was opened after the discharge-current peculiarity (the so-called current dip) with a chosen time delay ( $t_{\text{after dip}}$ ) in order to record optical spectra from different stages of the discharge, but the exposition time ( $t_{\text{exp}}$ ) was the same in all cases and amounted to  $1 \mu\text{s}$ . Similarly to the earlier studies,<sup>16</sup> the investigated discharges were observed by means of 3 fast photomultipliers placed behind 3 optical collimators, which were placed side-on the chamber at different distances from the electrodes outlets, at  $z = 16$  cm, 27 cm, and 40 cm, respectively. A scheme of this arrangement is shown in Fig. 1. Exemplary waveforms of the discharge current derivative ( $dI/dt$ ) and signals (OC) from the optical collimators and photomultipliers, which looked at the observed plasma region, are presented in Fig. 2.

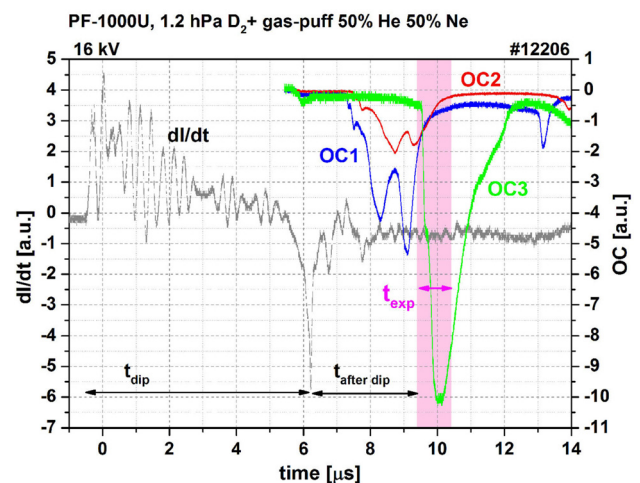


FIG. 2. Temporal shifts of the discharge current derivative ( $dI/dt$ ) peak and the signals from the optical collimators (OC), with the marked spectrometer exposition time ( $t_{\text{exp}}$ ). The values of  $t_{\text{after dip}}$  were changed for different discharges.

It should be noted that the duration of the emission of the jet, evaluated according to the OC signal, usually amounted to 1–2  $\mu\text{s}$ .

### III. EXPERIMENTAL RESULTS AND THEIR ANALYSIS

In all the reported experiments, the optical spectra were recorded from the volume having approximately the shape of a cylinder of (1–2) cm in diameter. The observation axis intersected the  $z$ -axis of the PF-1000U vacuum chamber at a distance of 16 cm or 27 cm from the outlets of the electrodes.

The composition of the recorded spectrum depended significantly on time of its exposition in relation to the jet arrival to the observation region. The spectra obtained before the jet arrival characterized only the background plasma, through which the plasma jet propagated. When the moment of the jet arrival corresponded to the spectrum recording period, the spectrum characterized both properties of background plasma and plasma in the dense jet. Since deuterium has the ionization potential equal to 13.6 eV, it was practically “burned out” (98% ionized). During the considered time period, its radiation characterized background plasma, through which the jet penetrated, as well as plasma surrounding the jet after its arrival. Furthermore, when registering spectra later, when the front of the jet has passed, but plasma remained after its passage has not yet been cooled, the deuterium lines are excited in the plasma surrounding the jet at some distance from it.

As mentioned earlier, the investigated discharges were carried out in different gases and their mixtures. In general, the chosen gas mixture was used in order to determine general characteristics of the jet distribution and the reliability of measurements of plasma parameters by means of the spectral lines of the chosen elements. Since the propagation velocity of the plasma flow at different gas conditions might differ significantly, the optical signals from the light collimators were used to adjust the starting moment of the spectrum recording. The analysis of the obtained data allowed the moment of the jet arrival (in the observation field) to be adjusted. Values of such a time-delay, averaged over the whole series of shots performed at different conditions, are given in Table I.

Table I shows that during the described experiments the time of the jet arrival (to the plane  $z = 27$  cm), as averaged over discharges performed at different gas conditions in the PF-1000U facility, changed from 1.11  $\mu\text{s}$  to 1.88  $\mu\text{s}$ , except for the shots performed at the initial pressure (0.53 hPa  $\text{D}_2$  + 0.13 hPa Ne) and the additional puffing of pure Ne, when it amounted to  $>3.0$   $\mu\text{s}$ . It should, however, be noted that in the mentioned experiments, as well as in those performed with the pure Ne filling, it was impossible to obtain a good plasma compression.

The data obtained from optical collimators were also used to determine an average speed of the jet front on the basis of time-of-flight observations. A considerable error was, however, made especially during measurements at short distances, because there was a big uncertainty in determining the place of the jet generation (within the length of a pinch column which spread over more than 10 cm) and the instant

TABLE I. Values of the mean time-delay (in  $\mu\text{s}$ ) between the current dip and jet arrival, as determined for different gas conditions.

Experimental conditions	$z = 16$ cm	$z = 27$ cm
Initial pressure 1.2 hPa $\text{D}_2$ + puffing of pure He	0.92	1.73
Initial pressure 1.2 hPa $\text{D}_2$ + puffing of (50% He + 50% Ne)	1.04	1.75
Initial pressure 1.2 hPa $\text{D}_2$		1.09
Initial pressure (1.06 hPa $\text{D}_2$ + 0.11 hPa He)		1.11
Initial pressure (1.06 hPa $\text{D}_2$ + 0.11 hPa He) + puffing of pure $\text{D}_2$		1.66
Initial pressure (1.06 hPa $\text{D}_2$ + 0.11 hPa He) + puffing of pure Ne		1.78
Initial pressure (0.53 hPa $\text{D}_2$ + 0.13 hPa Ne)		1.88
Initial pressure (0.53 hPa $\text{D}_2$ + 0.13 hPa Ne) + puffing of pure Ne		$>3.0$

of the jet generation. More accurate information was obtained by using two closely spaced collimators. Taking into account a time shift between the signals from the two measuring channels, it was possible to determine the actual instantaneous speed of the plasma jet in the observation plane. Averaged values of the instantaneous jet velocity, which were obtained from measurements performed at different distances from the electrode outlets, are shown in Fig. 3.

In the analysis of the results obtained at the stationary gas filling, all data from experiments performed with pure deuterium as well as those carried out with deuterium and 10%-admixture of helium were used. The results presented for the gas puffing were also summarized over experiments performed with different variants of the additional gas puffing (described earlier). From the data presented in Fig. 3, it follows that the jet velocity observed in discharges with the additional gas puffing was evidently lower than that in discharges at the stationary gas filling. This difference was

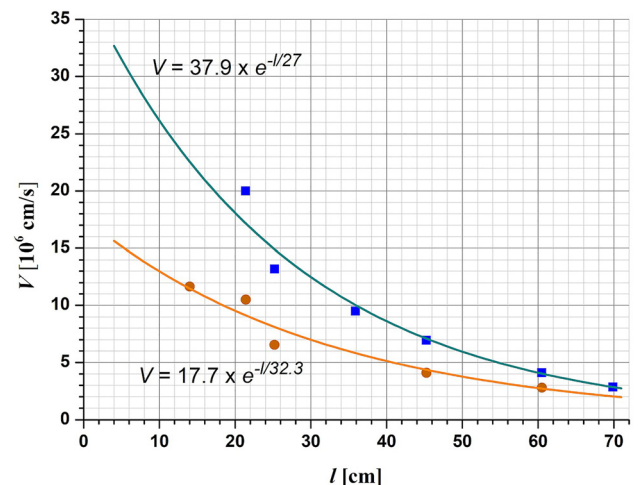


FIG. 3. Dependence of the instantaneous jet speed ( $V$ ) on a distance ( $l$ ) from the electrodes outlet plane, which was determined from measurements: ■ – at the stationary initial pressure equal to 1.2 hPa  $\text{D}_2$ , ● – at the additional gas puffing.

probably caused by more difficult penetration of the jet through a denser medium, which resulted from the injection of the additional gas during the formation of the jet and its propagation. It should here be noted that the experimental points in Fig. 3 could be approximated by the function  $V = V_0 \exp(-l/l_0)$ , where  $V_0$  is the initial velocity of the jet and  $l_0$  is the observed length of its dissipation. The results of the described measurements are given in Table II.

From Table II, it can be seen that for all the investigated shots in the PF-1000U facility, except for the previously mentioned Ne-discharges performed at the pure Ne-filling, the observed plasma jets achieved high velocity ranging up to about  $4 \times 10^7$  cm/s, which correspond to the typical velocity of jets emitted from young stellar objects.

The first series of discharges (#12197–#12201) was carried out at the initial filling of the PF-1000U chamber with pure  $D_2$  up to the pressure  $p_0 = 1.2$  hPa and the additional puffing of pure He. The optical spectra were recorded in the plane  $z = 16$  cm from the electrode outlets, at the chosen instants before and after the jet arrival. The described optical spectra are presented in Fig. 4.

To analyze the results of OES measurements, techniques described in the well known books and original papers were used.<sup>21–24</sup> The profiles of the recorded spectral lines were approximated by a Voigt function and values of the linear Stark broadening were determined, taking into account a dependence of the instrumental width on the wavelength. Intensities of some selected spectral lines were also measured. The known formulae describing a dependence of the Stark broadening  $\Delta_S \lambda$  of the  $D_\gamma$  433.9 nm line on the electron density, as well as diagrams showing a dependence of the intensity ratio of *He II* 468.6 nm and *He I* 587.6 nm on the electron temperature, was used.<sup>21,22</sup>

The analysis of the recorded spectra made it possible to estimate values of electron density and temperature. The results of this analysis for the first series of discharges are presented in Table III.

In Fig. 4, one can see that the intensity of some spectral lines was increased hundreds times when a plasma stream reached the observation plane at  $z = 16$  cm (see shots #12197

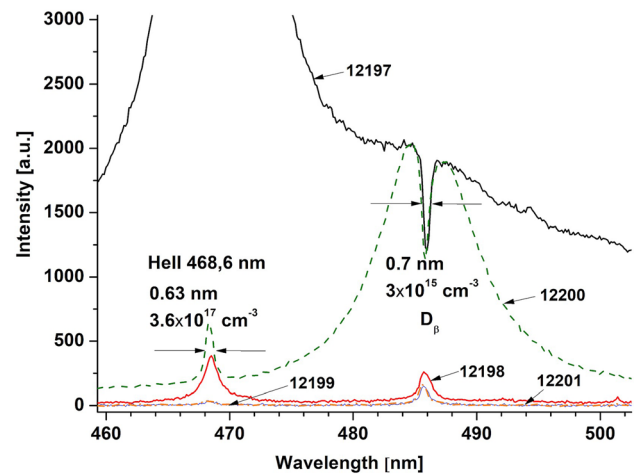
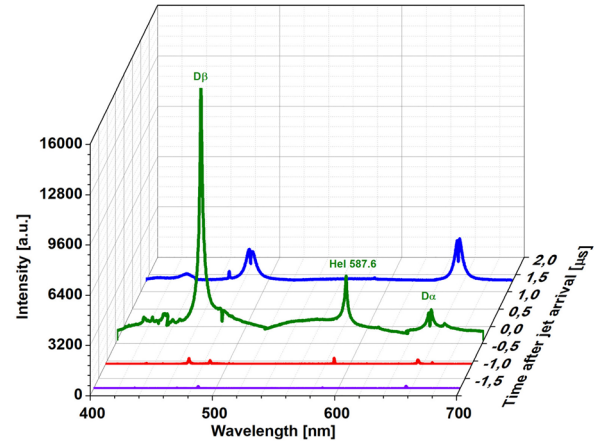


FIG. 4. Optical spectra of plasma generated in the PF-1000U facility after its filling with pure  $D_2$  and puffing of pure He, recorded with the exposition time of  $1 \mu\text{s}$  and presented as a function of a time delay of the plasma jet arrival to the observation plane (top), and an extended part of these spectra showing two distinct lines with corresponding HWHM values and computed electron densities (bottom).

TABLE II. Initial speed of the jet and the length of its dissipation.

Experimental conditions	$V_0$ $10^6$ (cm/s)	$l_0$ (cm)
Initial pressure 1.2 hPa $D_2$ + puffing of pure He	20.4	28.6
Initial pressure 1.2 hPa $D_2$ + puffing of (50%He + 50%Ne)	20.3	23.8
Initial pressure 1.2 hPa $D_2$	38.3	26.3
Initial pressure (1.06 hPa $D_2$ + 0.11 hPa He)	22.9	41.7
Initial pressure (1.06 hPa $D_2$ + 0.11 hPa He) + puffing of pure $D_2$	15.6	34.5
Initial pressure (1.06 hPa $D_2$ + 0.11 hPa He) + puffing of pure Ne	19.7	27.0
Initial pressure (0.53 hPa $D_2$ + 0.13 hPa Ne)	Not measured	...
Initial pressure (0.53 hPa $D_2$ + 0.13 hPa Ne) + puffing of pure Ne	5.5	166.7

and 12200). The spectrum from shot #12197 corresponded to the arrival of a front of the plasma stream, which had a high electron density ( $6 \times 10^{17} \text{ cm}^{-3}$ ) and an electron temperature slightly higher in a comparison with that measured during earlier instants. In optically thick plasma, there appears an additional broadening of spectral lines, and (depending on the whole number of the corresponding ions) the spectral lines can be broadened differently at the same plasma density. Therefore, for correct measurements of plasma parameters, it should be transparent for the considered spectral line. Unfortunately, in the reported experiments, it was not the case, as one can deduce from the recorded *He II* 468.6 nm and *He I* 587.6 nm lines. Before the plasma stream arrival, the broadening of the first line suggested that the electron density was four times higher than that calculated from the second line, what can be explained by its strong self-absorption. For a rough estimate of the maximal electron density, one might take the lower value calculated on the basis of the spectral lines mentioned earlier. However, taking into consideration the results of the subsequent experimental

TABLE III. Data obtained from shots performed at the initial filling with pure  $D_2$  and injection of pure He. The spectra were measured with the exposition time of  $1 \mu s$ . The Stark broadening  $\Delta_S \lambda$  of the  $D_\beta$  line shows the electron density of plasma surrounding the jet. The last two columns show the electron temperature ( $T_e$ ) and electron concentration ( $n_e$ ) of paraxial plasma, as determined taking into account self-absorption of the recorded spectral lines.

Time to jet arrival ( $\mu s$ )	Shot No.	From $D_\beta$ 485.5 nm		From $He II$ 468.6 nm		From $He I$ 587.6 nm		Ratio of $He II$ to $He I$	$T_e$ (eV)	$n_e$ $10^{17}$ ( $cm^{-3}$ )
		$\Delta_S \lambda$ (nm)	$n_e$ $10^{16}$ ( $cm^{-3}$ )	$\Delta_S \lambda$ (nm)	$n_e$ $10^{17}$ ( $cm^{-3}$ )	$\Delta_S \lambda$ (nm)	$n_e$ $10^{17}$ ( $cm^{-3}$ )			
-1.9	12201	0.80	0.6	1.2	8	0.33	2	2.2	4.4	0.6
-1.8	12199	0.83	0.7	1.3	8	0.32	2	2.15	4.4	0.6
-1.1	12198	1.20	1.2	1.6	10	0.44	3	4.5	4.7	1
-0.4	12197	0.53	0.3	3.5	20	3.1	20	8	5	6
+1.3	12200	0.62	0.3	0.63	3.6	0.47	3	11	5.1	1

series, when estimations were possible on the basis of helium- and neon-lines, the value determined from the  $He I$  587.6 nm line in the described experiments appeared to be overestimated about three times. Therefore, for shots #12197–12201, the last column in Table III gives the corrected values of the electron density (about three times lower than those obtained from the  $He I$  587.6 nm line).

A tail of the plasma stream, which was observed after passing the plasma front, appeared to remain still relatively hot (see data from shot #12200), but it was 5–6 times less dense than the main stream. It should be noted that the considered helium-lines were recorded even  $1.9 \mu s$  before the jet arrival. It could be explained by features of the gas-puffing system, which was triggered about 1.5 ms before the main discharge initiation. Simple estimates showed that before the formation of the dense pinch column, a cloud of the earlier puffed gas could expand up to a distance of about 20 cm, i.e., some helium could reach the observation plane, while the electron density amounted to about  $2 \times 10^{17} cm^{-3}$  and the electron temperature was sufficiently high (about 4.5 eV). On the other hand, it indicated the complete ionization of deuterium. In fact, the recorded profile of the  $D_\beta$  line did not characterize deuterium plasma (ionized by x-rays from a dense plasma focus), but its surrounding where the electron density was considerably lower ( $n_e = 6 \times 10^{15} cm^{-3}$ ). Consequently, during the jet arrival to the observation plane (see data from shots #12197 and 12200), the recorded deuterium-lines have also characterized plasma surrounding the axial jet. Those lines appeared to be re-absorption ones on the background of the intense emission of the quasi-axial plasma stream. The estimates of plasma parameters as a function of time, which took into account the effects considered above, are presented in Fig. 5.

It should here be noted that a good reproducibility of the experimental data obtained at almost the same time delays (shots #12199 and 12201) showed that the PF-1000U facility operated in a reproducible way, and a series of the similar experiments enabled the plasma parameters as a function of time to be determined quite exactly.

The second series of discharges (#12202–12209) was carried out at the initial filling of the PF-1000U chamber with pure  $D_2$  up to the pressure  $p_0 = 1.2$  hPa, but in contrast to the first series the puffing of a mixture (50% He + 50% Ne) was applied. The OES measurements in this series, as well as in all subsequent experiments, were performed at a distance of  $z = 27$  cm from the electrode outlets. Selected

parts of the optical spectra recorded for 3 different discharges are presented in Fig. 6.

Characteristic waveforms from shot #12207, which was performed at the identical gas conditions, are shown in Fig. 2, and a detailed analysis of two neon-lines recorded for this shot is presented in Fig. 7.

The results of a quantitative analysis of the considered second series of discharges are presented in Table IV and in Fig. 8.

During the second series of discharges and OES measurements at  $z = 27$  cm, a scenario observed for the first series of experiments was repeated. Before the arrival of the main plasma stream, the spectral lines emitted by excited atoms and ions of helium showed a relatively high electron temperature (3.8–3.9 eV) and some weak neon lines were recorded. The  $Ne II$  lines became much more intense after the plasma jet arrival (see shot #12202). At that instant, the intensity of the  $He$ -lines was increased about two orders of magnitude, and the re-absorption of these lines was also increased considerably, which made it impossible to determine accurately an electron density from their broadening. In contrast, the intensity of the  $D_\beta$  line (which corresponded to plasma surrounding the jet) was decreased, which indicated a burn-out of deuterium atoms. At this stage, the  $Ne II$  443.1 and 429.04 nm lines, which were characterized by a strong Stark broadening comparable with the instrumental width at  $n_e = 10^{17} cm^{-3}$  and a small re-absorption effect, were used for the determination of electron densities. The

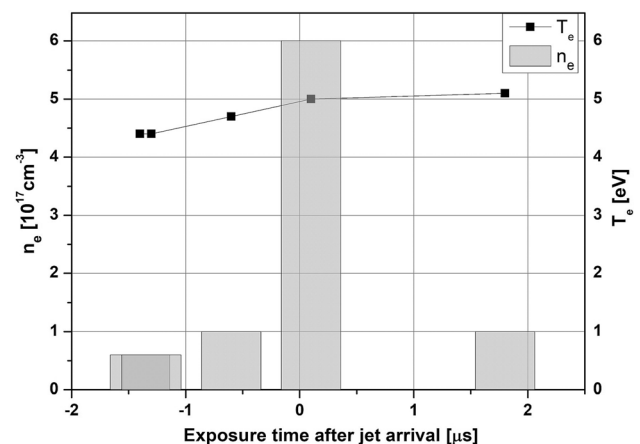


FIG. 5. Basic plasma parameters during the propagation of a plasma stream observed in experiments with the initial  $D_2$ -filling and additional puffing of pure He.

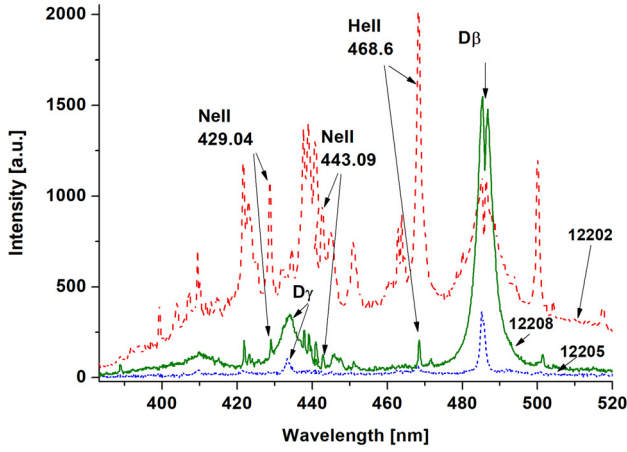


FIG. 6. Chosen parts (380–520 nm) of the optical spectra recorded in PF-1000U for a plasma stream generated in three discharges with the initial  $D_2$ -filling and additional puffing of a mixture (50% He + 50% Ne).

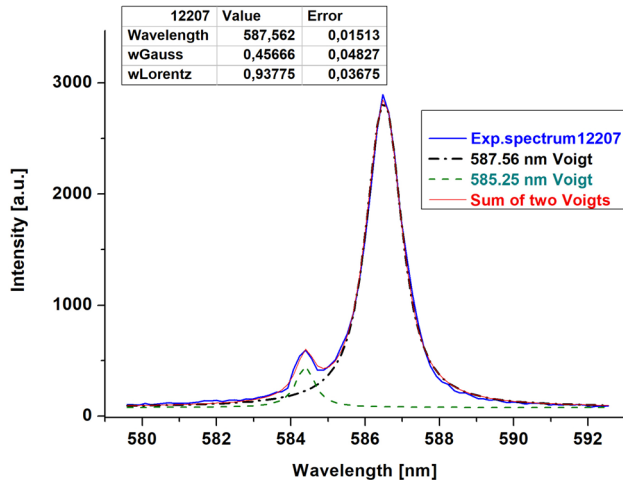


FIG. 7. Profiles of the  $Ne I$  585.25 nm and  $Ne I$  587.56 nm lines, which were recorded for shot #12207 and approximated by the Voigt functions. The Gaussian part of the fitting function corresponded to the spectrometer characteristics, and the Lorentz part—to the Stark broadening of the lines. The corresponding HWHM values are given in the upper inset.

electron density values, which were determined on the basis  $He$ -lines for shots #12202 and 12206, were overestimated 2–3 times in a comparison with those determined from the  $Ne II$  lines.

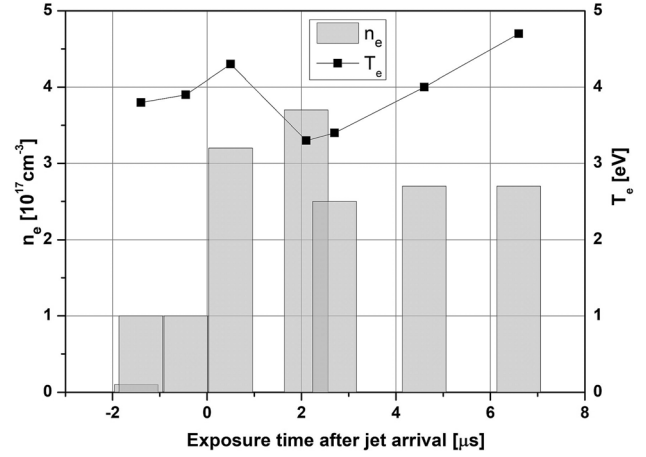


FIG. 8. Basic plasma parameters during the propagation of a plasma stream observed in experiments with the initial  $D_2$ -filling and additional puffing of a (He + Ne) mixture. Some increase in the plasma parameters during the period of 5–7  $\mu s$  was probably induced by the second pinching of a plasma focus column.

In a comparison with the first series of discharges, when the optical spectra were recorded at a distance  $z = 16$  cm, the second series of OES measurements at a distance  $z = 27$  cm showed that the electron temperature was lowered from about 5 eV to about 4 eV. Before the plasma jet arrival, the electron density was at a level of  $10^{17} \text{ cm}^{-3}$ , and the electron temperature (estimated by means of a “helium thermometer”) was 3.9 eV. During this phase, the electron density of the surrounding deuterium-plasma was about  $10^{16} \text{ cm}^{-3}$  only. This fact confirmed that (in both series of discharges) before the jet arrival the deuterium lines characterized the plasma cylindrical layer around the central jet, and the plasma parameters at the  $z$ -axis were considerably higher. At  $z = 27$  cm, the electron density in the jet and its tail amounted to about  $3 \times 10^{17} \text{ cm}^{-3}$  during about 6  $\mu s$ , and it was about two times lower than that measured at  $z = 16$  cm. It should, however, be mentioned that in the second series of discharges noticeable second pinches were observed, which appeared about 3–4  $\mu s$  after the first pinching. It could explain some increase in the plasma parameters in the period of 5–7  $\mu s$  after the jet arrival (see Fig. 8).

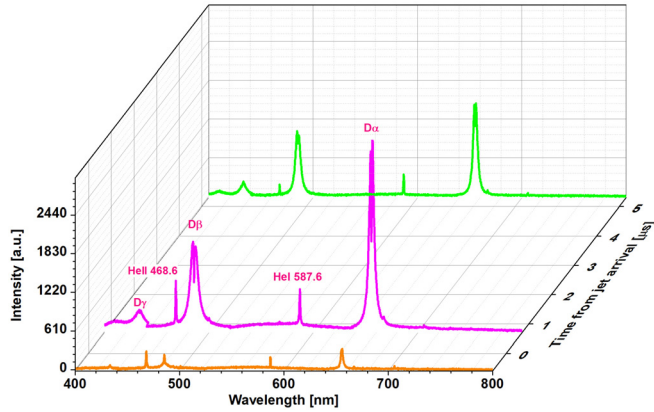
The third series of discharges (shots #12211–12214) was carried out at the initial filling of the PF-1000U chamber with a pure  $D_2$  up to the pressure  $p_0 = 1.2 \text{ hPa } D_2$  with no

TABLE IV. Data obtained from shots performed in the PF-1000U facility at the initial pure- $D_2$  filling and an additional puffing of a (50% He + 50% Ne) mixture. The electron density values determined on the basis of the  $Ne II$  443.1 nm line seem to be the most reliable ones.

Time to jet arrival ( $\mu s$ )	Shot No.	From $D_\beta$ 485.5 nm		From $Ne II$ 443.1 nm		From $He I$ 587.6 nm or $He II$ 468.6 nm		Ratio of $He II$ to $He I$	$T_e$ (eV)
		$\Delta_S \lambda$ (nm)	$n_e 10^{17} (\text{cm}^{-3})$	$\Delta_S \lambda$ (nm)	$n_e 10^{17} (\text{cm}^{-3})$	$\Delta_S \lambda$ (nm)	$n_e 10^{17} (\text{cm}^{-3})$		
-2.0	12203	1.1	0.1						
-1.9	12205	1.3	0.12			0.26/0.85	1.5/4.7	0.32	3.8
-0.95	12204	1.34	0.13			0.25/1.1	1.5/6	0.44	3.9
0	12202			0.67	3.2	1.5/1.55	8/10	1.43	4.3
+1.6	12206			0.77	3.7	1.57/0.44	8/2.3	0.03	3.3
+2.2	12207			0.51	2.5	0.94/0.23	5/1.8	0.04	3.4
+4.1	12208			0.56	2.7	0.69/0.38	3.2/2.2	0.63	4.0
+6.1	12209			0.57	2.7	0.54/0.63	3/3.6	4.3	4.7

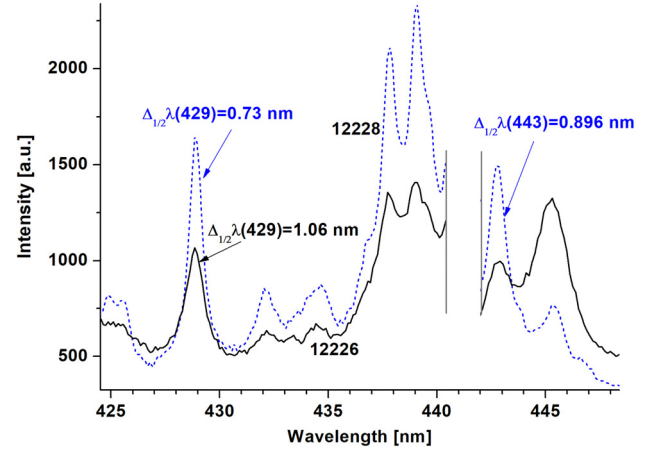
TABLE V. Data obtained from discharges performed at the initial filling of the PF-1000U chamber with pure D<sub>2</sub> without any additional gas puffing.

Shot No.	Time to jet arrival ( $\mu\text{s}$ )	From D <sub><math>\gamma</math></sub> 433.9 nm	
		$\Delta_S \lambda$ (nm)	$n_e$ 10 <sup>17</sup> (cm <sup>-3</sup> )
12211	-0.8	1.13	0.14
12212	+2.2	8.53	1.8
12213	+5.2	5.85	1
12214	+8.3	4.1	1

FIG. 9. Optical spectra of plasma generated in the PF-1000U facility after its filling with a (D<sub>2</sub> + He) mixture up to pressure  $p_0 = (1.06 \text{ hPa D}_2 + 0.11 \text{ hPa He})$  with no additional gas puffing.

additional gas-puffing. Because of the strong re-absorption of deuterium lines, for estimates of the plasma parameters, only the D <sub>$\gamma$</sub>  line was used. In the first experiment (shot #12211), which concerned the situation before the plasma stream arrival, the electron density of plasma surrounding the axis was estimated, which was equal to  $1.4 \times 10^{16} \text{ cm}^{-3}$ . The OES measurements in three subsequent experiments also provided the maximal estimates of plasma surrounding the central stream, because deuterium inside the jet was completely ionized. This observation resulted from the previous experimental series, when a small admixture of helium was applied for diagnostic purposes, and the electron temperature amounted to 4 eV. The values of the electron density, as estimated for plasma surrounding the main jet, are presented in Table V.

The fourth series of discharges (shots #12215–12217) was carried out at the initial filling of the PF-1000U chamber with a (D<sub>2</sub> + He) mixture up to the pressure  $p_0 = 1.06 \text{ hPa D}_2 + 0.11 \text{ hPa He}$ , but no additional gas-puffing was applied. The optical spectra, which were recorded also at a distance

FIG. 10. Profiles of the Ne II 429.0 nm and Ne II 443.09 nm from a neon-plasma stream generated in the PF-1000U facility operated at the (D<sub>2</sub> + 10% He) filling and puffing of Ne.

$z = 27 \text{ cm}$ , are presented in Fig. 9, and the results of their analysis are summarized in Table VI.

In this short series of discharges, carried out at the initial stationary filling of the chamber with a (D<sub>2</sub> + 10%He) mixture, the electron density of plasma produced before the jet propagation was  $< 2.5 \times 10^{16} \text{ cm}^{-3}$ , as estimated on the basis of the D <sub>$\gamma$</sub>  line from shot #12216. The electron density in the main plasma jet, as estimated from the He-lines from shots #12215 and 12217, amounted to  $4 \times 10^{17} \text{ cm}^{-3}$ , but it could be slightly overvalued because of some re-absorption effects. The electron temperature in the plasma stream and its tail decreased from about 4.7 eV to 4.0 eV. Deuterium inside the plasma jet was of course completely ionized. Therefore, the D <sub>$\gamma$</sub>  from shot #12217 provided only the maximal value of the electron density in plasma surrounding the central jet.

The next series of discharges (shots #12226–12232) was performed at the initial filling of the PF-1000U chamber with a (D<sub>2</sub> + 10% He) mixture up to the pressure  $p_0 = (1.06 \text{ hPa D}_2 + 0.11 \text{ hPa He})$  and an additional puffing of pure Ne. The selected parts of the optical spectra, which were recorded for two chosen discharges, are presented in Fig. 10.

The results of an analysis of all the optical spectra, which were recorded in the considered series of experiments, are given in Table VII.

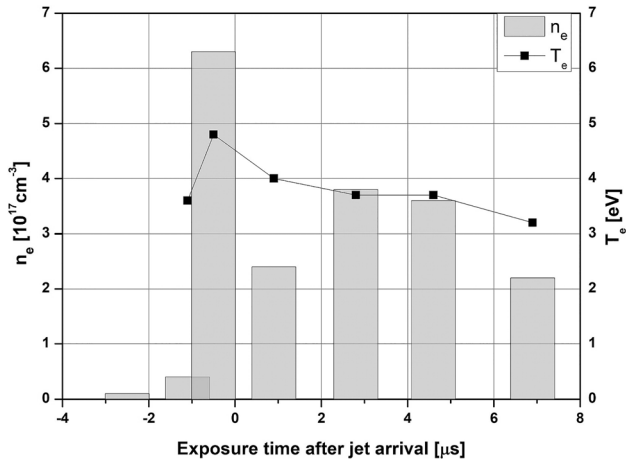
In this series of discharges before the plasma stream arrival to the observation plane, i.e., at time delays  $< 1 \mu\text{s}$ , it was possible to record intense deuterium lines and weak helium lines. The electron density in surrounding plasma, as estimated from broadening of the D <sub>$\beta$</sub>  line, was about

TABLE VI. Data obtained from discharges performed at the initial filling of the PF-1000U chamber up to the pressure  $p_0 = (1.06 \text{ hPa D}_2 + 0.11 \text{ hPa He})$  with no additional gas puffing.

Time to jet arrival ( $\mu\text{s}$ )	Shot No.	From D <sub><math>\gamma</math></sub> 433.9 nm		From HeII 468.6 nm		From HeI 587.6 nm		Ratio of He II to He I	$T_e$ (eV)
		$\Delta_S \lambda$ (nm)	$n_e$ 10 <sup>17</sup> (cm <sup>-3</sup> )	$\Delta_S \lambda$ (nm)	$n_e$ 10 <sup>17</sup> (cm <sup>-3</sup> )	$\Delta_S \lambda$ (nm)	$n_e$ 10 <sup>17</sup> (cm <sup>-3</sup> )		
-0.6	12216	2.1	0.25	0.42	2.4	0.24	1.5	3.9	4.75
+0.7	12215			0.7	4	0.9	4	1.18	4.25
+5.3	12217	5.5	1	0.88	5	0.55	3	0.57	4.0

TABLE VII. Data obtained from discharges performed at the initial filling of the PF-1000U chamber with the ( $D_2 + 10\%$  He) mixture and the application of an additional puffing of Ne.

Shot No.	Time to jet arrival ( $\mu\text{s}$ )	From $D_\beta$ 485.5 nm, $Ne II$ 443.09 nm or $Ne II$ 429.0 nm		From $He II$ 468.6 nm		From $He I$ 587.6 nm		Ratio of $He II$ to $He I$	$T_e$ (eV)
		$\Delta_S \lambda$ (nm)	$n_e, 10^{17} (\text{cm}^{-3})$	$\Delta_S \lambda$ (nm)	$n_e, 10^{17} (\text{cm}^{-3})$	$\Delta_S \lambda$ (nm)	$n_e, 10^{17} (\text{cm}^{-3})$		
12227	-3.0	1.00	( $D_\beta$ ) 0.09	...	...	...	...	...	...
12229	-1.6	1.00	( $D_\beta$ ) 0.10	0.1	0.4	0.15	0.8	0.1	3.6
12226	-1.0	1.06	(429) 6.3	1.08	6	0.55	3	5.4	4.8
12230	+0.4	0.4	(429) 2.4	0.48	2.4	1.42	8	0.52	4.0
12228	+2.3	0.65	(429) 3.8	0.9	5	1.17	7	0.14	3.7
12231	+4.1	0.76	(443) 3.6	0.31	2.1	0.37	2	0.17	3.7
12232	+6.4	...	...	0.36	2.2	0.41	2.3	0.02	3.2

FIG. 11. Parameters of a plasma stream produced in experiments performed at the initial filling with a ( $D_2 + 10\%$  He) mixture and the application of the additional Ne-puffing.

$10^{16} \text{ cm}^{-3}$ . In shot #12226, the front of the arriving plasma stream was probably recorded, which had the electron density equal to  $6.3 \times 10^{17} \text{ cm}^{-3}$  and the electron temperature increased to 4.8 eV. After the plasma jet arrival, the intensity of the  $He I$  587.6 nm line was increased about 100 times, the radiation of deuterium was decreased, and the radiation of neon appeared. The electron density in the main plasma stream, as estimated from the broadening of the  $Ne II$  and  $He II$  lines, amounted to  $(3-4) \times 10^{17} \text{ cm}^{-3}$ , and the electron temperature of the stream tail was decreased to about (3–4) eV.

The plasma parameters described earlier, which were obtained from the fifth series of experiments, are compared in Fig. 11.

The last series of discharges (#12235–12238) was carried out at the initial filling of the PF-1000U chamber with a ( $D_2 + Ne$ ) mixture up to the pressure  $p_0 = (0.53 \text{ hPa } D_2 + 0.13 \text{ hPa } Ne)$ , which was equal to about half of that applied in the previous experiments. Two discharges were performed without any additional gas-puffing, and two other with the additional puffing of Ne. The plasma parameters, which were obtained from the last series, are presented in Table VIII.

During 2.5  $\mu\text{s}$  period before the plasma stream arrival (shot #12237), there was no emission of the  $Ne II$  line. The electron density in the plasma surrounding the axial region, as estimated from the  $D_\beta$  broadening, was about  $3 \times 10^{15} \text{ cm}^{-3}$ . In three other shots, all deuterium Balmer lines were considerably broadened due to the re-absorption effects. Therefore, in those discharges for estimates of electron densities in the plasma stream, the  $Ne II$  lines were used, but estimations based on the  $Ne II$  429 nm line were inaccurate because of its very narrow shape.

The estimations of the electron density in the plasma stream and its tail, as performed on the basis of the  $Ne II$  443 nm line, gave the values equal to about  $3 \times 10^{17} \text{ cm}^{-3}$ . It should be added that the maximal intensity of the optical spectra recorded in the considered series of experiments was about two times lower than that observed in the previous experimental series. In the recorded optical spectra, no distinct differences were observed for shots with and without additional Ne-gas injection, but the number of discharges was too small in order to make a credible conclusion.

It should be mentioned that additional short series of discharges were also performed at other gas conditions, as shown in Tables I and II, but their results did not appear to

TABLE VIII. Data obtained in experiments performed at initial filling of the PF-1000U chamber with a mixture ( $D_2 + Ne$ ), without and with additional Ne puffing.

Shot No.	Gas-puffing	Time to jet arrival ( $\mu\text{s}$ )	From $D_\beta$ or $D_\gamma$		From $Ne II$ 443 nm	
			$\Delta_S \lambda$ (nm)	$n_e 10^{17} (\text{cm}^{-3})$	$\Delta_S \lambda$ (nm)	$n_e, 10^{17} (\text{cm}^{-3})$
12237	Ne	-3.5	0.5	0.03 ( $D_\beta$ )		
12235	None	-0.4			0.64	3.1
12236	None	+1.3			0.60	2.9
12238	Ne	+2.2	2.7	0.4 ( $D_\gamma$ )	0.61	3.0

be worth of detailed descriptions, except for some data to be presented in summary.

#### IV. SUMMARY AND CONCLUSIONS

The most important results of the described studies can be summarized as follows: The OES measurements were performed within the PF-1000U facility at distances of 16 cm and 27 cm from the electrode outlets, i.e., at distances much smaller than those observed during the preliminary studies.<sup>16</sup> The investigated discharges were carried out at various gas conditions and at different instants after the current peculiarity (dip), which corresponded to the maximum compression of a current sheath,<sup>25</sup> i.e., the instant of a dense plasma-focus column formation and the generation of a plasma jet. The recorded optical spectra were carefully analyzed using the known spectroscopic techniques,<sup>21–24</sup> and electron densities as well as electron temperatures were estimated. The obtained results enabled a comparison to be performed, as presented in Table IX.

It should be noted here that even before the arrival of the plasma jet it was possible to estimate an electron density and electron temperature of primary plasma, and that the effect was independent of the application of an additional gas injection. Apparently, near the  $z$ -axis, a helium-plasma column had a relatively high electron density (about  $10^{17} \text{ cm}^{-3}$ ) and its electron temperature was high enough (3.6–4.4 eV) to ensure the full ionization of deuterium. In this discharge phase, the electron density in deuterium plasma, which surrounded the helium-plasma core, was ten times lower (about  $10^{16} \text{ cm}^{-3}$ ).

With the jet arrival to the observation plane, the intensity of the observed optical spectra was increased about two orders of magnitude. The data presented in Table IX show that a dependence of the electron density in environmental plasma on the investigated gas conditions was rather weak, but 10% admixture of He or 25% admixture of Ne (added to the  $D_2$ -filling) caused an increase in the  $n_e$  values by factor (1.8–2.5). In all the investigated cases, the electron density in plasma jets was about one order of magnitude higher than that in the plasma surrounding. When the additional injection

of He or Ne was applied, the electron density in the plasma jet amounted to  $(2–6) \times 10^{17} \text{ cm}^{-3}$ . At a larger distance from the electrodes outlets (i.e., at  $z = 27 \text{ cm}$ , instead of  $z = 16 \text{ cm}$ ), the electron temperature in the plasma jet was decreased (from 5 eV to 4.5 eV), and the electron density was reduced by about a half value.

The electron temperature of the plasma tail had also slowly decreased, approximately 1.5 times (from 4.5 eV to 3 eV) in about 6  $\mu\text{s}$ . These values did not differ significantly from those identified in the preliminary studies.<sup>16</sup> During those earlier measurements, which were performed at a distance of 57 cm from the electrodes outlets, the maximum electron temperature (estimated with a “helium thermometer”) amounted to 5.3 eV, but the electron density was several times lower ( $< 10^{17} \text{ cm}^{-3}$ ). It should, however, be noted that an accurate separation of the plasma environment from a relatively hot plasma jet (or its precursor) on the basis of the applied OES methods was impossible, and it requires the implementation of other diagnostic techniques.

One should remember here that relatively low  $T_e$  values, as determined from the described spectroscopic measurements, corresponded to the values averaged (during the exposition time) over the whole solid cone of the spectroscopic observations, and, namely, over the (1–2)-cm-diameter region of the plasma stream at the  $z$ -axis, relatively far from the electrodes outlets. The local  $T_e$  values might be much higher, particularly inside the dense plasma pinch column (plasma-focus), where many filaments and hot-spots were observed by means of soft x-ray diagnostics.<sup>26</sup>

Taking into account also the results of other measurements (particularly those of axial velocities of the plasma stream), it was concluded that dimensionless parameters of plasma jets produced during the reported studies were very similar to those given in the earlier publication.<sup>16</sup> Since the main observations were performed at a distance about two times smaller than that in the preliminary studies, the Mach number reached higher values  $M > 5$  and the density contrast ( $n_{\text{jet}}/n_{\text{ambient}}$ ) was  $> 10$ , the Reynolds number achieved the value of  $Re > 3 \times 10^4$ , and the Péclet number was  $Pe > 10^7$ . It means that the PF-1000U discharges at the described

TABLE IX. Parameters of ambient plasma and plasma jets as a function of gas-conditions. The symbols (He) and (D) indicate that the electron density values were determined from spectral lines of those elements.

Gas conditions	Electron density before jet arrival $\times 10^{16} \text{ (cm}^{-3}\text{)}$	Electron temperature before jet arrival (eV)	Electron density in jet $n_e \times 10^{17} \text{ (cm}^{-3}\text{)}$	Electron temperature in plasma jet $T_e \text{ (eV)}$	Electron density in plasma surround. jet $\times 10^{16} \text{ (cm}^{-3}\text{)}$
1.2 hPa $D_2$ + puffing of He	At $z = 16 \text{ cm}$ 10 (He) 1.2 (D)	4.4	7	4.7–5.1	0.3
1.2 hPa $D_2$ + puffing of (50% He+50% Ne)	At $z = 27 \text{ cm}$ 15 (He) 0.6 (D)	3.8	3	4.3–4.7	Not measured
1.2 hPa $D_2$ + no puffing	At $z = 27 \text{ cm}$ 1.4 (D)	Not measured	Not measured	Not measured	10
(1.06 hPa $D_2$ + 0.11 hPa He) + no puffing	At $z = 27 \text{ cm}$ 15 (He) $< 2.5$ (D)	Not measured	4	4.7	10
(1.06 hPa $D_2$ + 0.11 hPa He) + puffing of Ne	At $z = 27 \text{ cm}$ 15 (He) 1.0 (D)	3.6	2–6	4.8	Not measured
(0.53 hPa $D_2$ + 0.13 hPa Ne) + no puffing	At $z = 27 \text{ cm}$ not measured	Not measured	3	$> 3.5$	Not measured
(0.53 hPa $D_2$ + 0.13 hPa Ne) + puffing of Ne	At $z = 27 \text{ cm}$ 0.3 (D)	Not measured	3	$> 3.5$	Not measured

gas-conditions and, in particular, shots with the additional gas-puffing might be used for astrophysical simulation experiments in a laboratory.

## ACKNOWLEDGMENTS

The authors acknowledge that the described studies were supported by the Russian Science Foundation (as a Project No. 16-12-10051) as well as the IAEA CRP (as a Contract No. 23071), and Polish national resources allocated to science in 2017 and awarded to support co-financed international collaborative projects at the IFPiLM.

- <sup>1</sup>J. Contopoulos, "A simple type of magnetically-driven jets: An astrophysical plasma gun," *Astrophys. J.* **450**, 616–627 (1995).
- <sup>2</sup>J. F. C. Wardle, D. C. Homan, R. Ojha, and D. H. Roberts, "Electron-positron jets associated with the Quasar 3C279," *Nature* **395**, 457–461 (1998).
- <sup>3</sup>K. Hirotani, S. Iguchi, M. Kimura, and K. Wajima, "Pair-plasma dominance in the parsec-scale relativistic jet of 3C345," *Astrophys. J.* **545**, 100–106 (2000).
- <sup>4</sup>R. K. Williams, "Collimated escaping vertical polar e-e+ jets intrinsically produced by rotating black holes and Penrose processes," *Astrophys. J.* **611**, 952–963 (2004).
- <sup>5</sup>S. You, G. S. Yun, and P. M. Bellan, "Dynamic and stagnating plasma flow leading to magnetic-flux-tube collimation," *Phys. Rev. Lett.* **95**, 045002 (2005).
- <sup>6</sup>L. Pavan, P. Bordas, G. Puhlhofer, M. D. Filipovic, A. De Horta, A. O. Brien, M. Balbo, R. Walter, E. Bozzo, C. Ferrigno, E. Crawford, and L. Stella, "The long helical jet of the Lighthouse nebula, IGR J1 1014-6103," *Astron. Astrophys.* **562**, A122 (2014).
- <sup>7</sup>J. H. Beall, "A review of astrophysical jets," *Acta Polytech. CTU Proc.* **1**, 259–264 (2015).
- <sup>8</sup>D. D. Ryutov and B. A. Remington, "Scaling astrophysical phenomena to high-energy-density laboratory experiments," *Plasma Phys. Controlled Fusion* **44**, B407–B423 (2002).
- <sup>9</sup>B. A. Remington, R. P. Drake, and D. D. Ryutov, "Experimental astrophysics with high power lasers and Z pinches," *Rev. Mod. Phys.* **78**, 755–807 (2006).
- <sup>10</sup>S. V. Lebedev, J. P. Chittenden, F. N. Beg, S. N. Bland, A. Ciardi, D. Ampleford, S. Hughes, M. G. Haines, A. Frank, E. G. Blackman, and T. Gardiner, "Laboratory astrophysics and collimated stellar outflows: The production of radiatively cooled hypersonic plasma jets," *Astrophys. J.* **564**, 113–119 (2002).
- <sup>11</sup>A. Ciardi, "Laboratory studies of astrophysical jets," *Lect. Notes Phys.* **793**, 31–50 (2010).
- <sup>12</sup>F. Suzuki-Vidal, S. V. Lebedev, M. Krishnan, M. Bocchi, J. Skidmore, G. Swadling, A. J. Harvey-Thompson, G. Burdiak, P. de Grouchy, L. Pickworth, L. Suttle, S. N. Bland, J. P. Chittenden, G. N. Hall, E. Khoory, K. Wilson-Elliott, R. E. Madden, A. Ciardi, and A. Frank, "Laboratory astrophysics experiments studying hydrodynamic and magnetically-driven plasma jets," *J. Phys.: Conf. Ser.* **370**, 0120002 (2012).
- <sup>13</sup>B. Albertazzi, A. Ciardi, M. Nakatsutsumi, T. Vinci, J. Béard, R. Bonito, J. Billette, M. Borghesi, Z. Burkley, S. N. Chen, T. E. Cowan, T. Herrmannsdörfer, D. P. Higginson, F. Kroll, S. A. Pikuz, K. Naughton, L. Romagnani, C. Riconda, G. Revet, R. Riquier, H.-P. Schlegelvoigt, I. Yu. Skoblev, A. Ya. Faenov, A. Soloviev, M. Huarte-Espinosa, A. Frank, O. Portugall, H. Pépin, and J. Fuchs, "Laboratory formation of a scaled proto-stellar jet by coaligned poloidal magnetic field," *Science* **346**, 325–328 (2014).
- <sup>14</sup>V. Krauz, V. Myalton, V. Vinogradov, E. Velikhov, S. Ananyev, S. Dan'ko, Y. Kalinin, A. Kharrasov, K. Mitrofanov, and Y. Vinogradova, "Adaptation of plasma focus type facilities for laboratory simulation of astrophysical jets," *EPS Conf. Plasma Phys.* **39E**, P4.401 (2015).
- <sup>15</sup>S. S. Ananyev, S. A. Dan'ko, V. V. Myalton, A. I. Zhuzhunashvili, Y. G. Klainin, V. I. Krauz, M. S. Ladygina, and A. K. Marchenko, "Spectroscopic measurements of the parameters of helium plasma jets generated in the plasma focus discharge at the PF-3 facility," *Plasma Phys. Rep.* **42**(3), 269–277 (2016).
- <sup>16</sup>E. Skladnik-Sadowska, S. A. Dan'ko, R. Kwiatkowski, M. J. Sadowski, D. R. Zaloga, M. Paduch, E. Zielinska, A. M. Kharrasov, and V. I. Krauz, "Optical spectroscopy of deuterium and helium jets emitted from plasma focus discharges at the PF-1000U facility," *Phys. Plasmas* **23**, 122902 (2016).
- <sup>17</sup>P. Kubes, M. Paduch, T. Pisarczyk, M. Scholz, T. Chodukowski, D. Klir, J. Kravarik, K. Rezac, I. Ivanova-Stanik, L. Karpinski, K. Tomaszewski, and M. J. Sadowski, "Interferometric study of pinch phase in a plasma-focus device at the time of neutron production," *IEEE Trans. Plasma Sci.* **37**, 2191–2196 (2009).
- <sup>18</sup>K. N. Mitrofanov, S. S. Anan'ev, D. A. Voitenko, V. I. Krauz, G. I. Astapenko, A. I. Markoliya, and V. V. Myalton, "Localization of the magnetic field in a plasma flow in laboratory simulations of astrophysical jets at the KPF-4-PHOENIX installation," *Astron. Rep.* **61**, 775–782 (2017).
- <sup>19</sup>S. A. Dan'ko, S. S. Ananyev, Y. G. Kalinin, V. I. Krauz, and V. V. Myalton, "Spectroscopic studies of the parameters of plasma jets during their propagation in the background plasma on the PF-3 facility," *Plasma Phys. Controlled Fusion* **59**, 045003 (2017).
- <sup>20</sup>K. N. Mitrofanov, V. I. Krauz, V. V. Myalton, E. P. Velikhov, V. P. Vinogradov, and Y. V. Vinogradova, "Magnetic field distribution in the plasma flow generated by a plasma focus discharge," *J. Exp. Theor. Phys.* **119**, 910–923 (2014).
- <sup>21</sup>H. R. Griem, *Plasma Spectroscopy* (McGraw-Hill, New York, 1964).
- <sup>22</sup>*Plasma Diagnostic Techniques*, edited by R. H. Huddleston and S. L. Leonard (Academic Press, New York, London, 1965).
- <sup>23</sup>H. R. Griem, *Spectral Line Broadening by Plasma* (Academic Press, New York, 1974).
- <sup>24</sup>N. Konjević, A. Lasage, J. R. Fuhr, and W. L. Wiese, "Experimental Stark widths and shifts of spectral lines of neutral and ionized atoms," *J. Phys. Chem. Ref. Data* **31**, 819 (2002).
- <sup>25</sup>M. J. Sadowski and M. Scholz, "The main issues of research on dense magnetized plasmas in PF discharges," *Plasma Sources Sci. Technol.* **17**, 024001 (2008).
- <sup>26</sup>E. Skladnik-Sadowska, D. Zaloga, M. J. Sadowski, R. Kwiatkowski, K. Malinowski, R. Miklaszewski, M. Paduch, W. Surala, E. Zielinska, and K. Tomaszewski, "Research on soft x-rays in high-current plasma-focus discharges and estimation of plasma electron temperature," *Plasma Phys. Controlled Fusion* **58**, 095003 (2016).